Enhanced Release of Glucose Into the Intraluminal Space of the Intestine Associated With Metformin Treatment as Revealed by [^{18}F]Fluorodeoxyglucose PET-MRI

Yasuko Morita,[1] Munenobu Nogami,[2] Kazuhiko Sakaguchi,[1] Yuko Okada,[1] Yushi Hirota,[1] Kenji Sugawara,[1] Yoshikazu Tamori,[1,3] Feibi Zeng,[2] Takamichi Murakami,[2] and Wataru Ogawa[1]

Diabetes Care 2020;43:1796–1802 | https://doi.org/10.2337/dc20-0093

OBJECTIVE

Positron emission tomography (PET)–computed tomography has revealed that metformin promotes the intestinal accumulation of [^{18}F]fluorodeoxyglucose (FDG), a nonmetabolizable glucose derivative. It has remained unknown, however, whether this accumulation occurs in the wall or intraluminal space of the intestine. We here addressed this question with the use of [^{18}F]FDG PET-MRI, a recently developed imaging method with increased accuracy of registration and high soft-tissue contrast.

RESEARCH DESIGN AND METHODS

Among 244 individuals with type 2 diabetes who underwent PET-MRI, we extracted 24 pairs of subjects matched for age, BMI, and HbA_{1c} level who were receiving treatment with metformin (metformin group) or were not (control group). We evaluated accumulation of [^{18}F]FDG in different portions of the intestine with both a visual scale and measurement of maximum standardized uptake value (SUV_{max}), and such accumulation within the intestinal wall or lumen was discriminated on the basis of SUV_{max}.

RESULTS

SUV_{max} of the jejunum, ileum, and right or left hemicolon was greater in the metformin group than in the control group. [^{18}F]FDG accumulation in the ileum and right or left hemicolon, as assessed with the visual scale, was also greater in the metformin group. SUV_{max} for the intraluminal space of the ileum and right or left hemicolon, but not that for the intestinal wall, was greater in the metformin group than in the control group.

CONCLUSIONS

Metformin treatment was associated with increased accumulation of [^{18}F]FDG in the intraluminal space of the intestine, suggesting that this drug promotes the transport of glucose from the circulation into stool.

[1]Division of Diabetes and Endocrinology, Department of Internal Medicine, Kobe University Graduate School of Medicine, Kobe, Japan
[2]Department of Radiology, Kobe University Graduate School of Medicine, Kobe, Japan
[3]Division of Creative Health Promotion, Department of Social/Community Medicine and Health Science, Kobe University Graduate School of Medicine, Kobe, Japan

Corresponding author: Wataru Ogawa, ogawa@med.kobe-u.ac.jp

Received 13 January 2020 and accepted 6 April 2020

This article contains supplementary material online at https://doi.org/10.2337/figshare.12106923.

Inhibition of hepatic gluconeogenesis, which appears to be achieved by multiple molecular mechanisms (1–4), is thought to be largely responsible for the glucose-lowering effect of metformin (5). In addition to this action in the liver, however, metformin likely exerts various effects on the gut that contribute to the lowering of blood glucose levels (6,7). Biguanides, the class of drugs to which metformin belongs, were thus shown long ago to inhibit the absorption of ingested glucose from the gut (8), an action that was recently confirmed by modern techniques (9). Metformin has also been shown to activate a gut-brain-liver circuit that leads to the suppression of hepatic glucose production (10). Although the detailed mechanisms remain incompletely understood, effects on the gut microbiota also likely play a role in the glucose-lowering action of metformin (11,12).

Positron emission tomography (PET)–computed tomography (CT) with ^{18}F-labeled fluorodeoxyglucose (FDG), a nonmetabolizable derivative of glucose, is adopted as an imaging method to detect malignant tumors, which tend to take up and consume larger amounts of glucose compared with normal tissues (13). Metformin was recently found to increase the accumulation of radioactivity in the intestine during [^{18}F]FDG PET-CT imaging (14–17). Given that metformin stimulates the uptake and utilization of glucose in the intestine in rodent models (16,18), it is possible that it exerts similar effects in humans and that the PET-CT images reflect the augmented accumulation of glucose in intestinal cells. In PET-CT, however, the images of the two methods are not obtained simultaneously but sequentially, which raises the possibility that bowel peristalsis during image acquisition might result in misregistration of CT and PET images. It has thus been difficult to determine in which compartment of the intestine—the intestinal wall or intraluminal space—the accumulation of [^{18}F]FDG occurs.

PET-MRI is a recently launched imaging method that consists of a state-of-the-art PET component integrated into an MRI scanner. The PET component is compatible with a strong magnetic field, which allows PET and MRI images to be acquired simultaneously for the same position of the patient (19,20), resulting in a higher precision of the fused images of the two methods compared with PET-CT (21). PET-MRI is thus superior to PET-CT with regard to interpretation of the combined images—in particular, for imaging of organs that move, such as the digestive tract (22,23). Moreover, MRI provides higher soft-tissue contrast than does CT, yielding detailed and comprehensive information on the contents and structure of the digestive tract (24,25).

We have now taken advantage of PET-MRI to investigate the intestinal compartment in which [^{18}F]FDG accumulates in subjects receiving or not receiving metformin treatment. Our results indicate that [^{18}F]FDG accumulates in the intraluminal space of the intestine and that this accumulation is augmented by metformin.

RESEARCH DESIGN AND METHODS

Study Subjects and Data Collection

This retrospective study was conducted in accordance with the Declaration of Helsinki and its amendments and was approved by the Kobe University Hospital Ethics Committee (approval no. B190023), Kobe, Japan. Among 1,246 individuals who underwent [^{18}F]FDG PET-MRI at Kobe University Hospital between April 2016 and August 2018, 244 were found to have type 2 diabetes, and 50 of these 244 individuals were receiving treatment with metformin (Supplementary Fig. 1). Of these 50 individuals, 5 were excluded on account of repeated PET-MRI examinations and 1 because of insufficient medical information. An additional 17 individuals, who had terminated metformin administration at least 48 h before the PET-MRI examination, were excluded given that such termination greatly diminishes the effect of metformin on the accumulation of [^{18}F]FDG in the intestine (26–28). The remaining 27 metformin-treated individuals and 194 nonmetformin-treated individuals with type 2 diabetes were matched for age, BMI, and HbA_{1c} on the basis of the logit of the propensity score with the use of the nearest-neighbor matching method without replacement at a caliper width of SD × 0.2.

PET-MRI Examination

Whole-body PET-MRI (Signa PET/MR; GE Healthcare, Waukesha, WI) was performed 60 min after intravenous administration of 2-[^{18}F]fluoro-2-deoxy-D-glucose (3.5 MBq/kg) without intravenous contrast material in subjects who fasted for at least 6 h. PET images were obtained by a routine method. In brief, a PET scan for the upper abdominal bed was performed for 5 min and was respiratory-gated by quiescent period gating (Q static) with offset and acquisition windows of 30% and 50%, respectively. The attenuation correction was made with the 2-point Dixon three-dimensional volumetric interpolated fast spoiled gradient echo (Dixon) acquired simultaneously under free breathing. The images were reconstructed by time-of-flight ordered subset expectation maximization with two iterations, 16 subsets, and a Gaussian filter of 4.0 mm with a point-spread function. MRI images were also obtained with a routine method. In brief, a T1-weighted Dixon image with respiratory gating and a T2-weighted single-shot fast-spin echo sequence were acquired simultaneously with the PET scan. Dixon is a three-dimensional dual-echo gradient echo sequence with a 2-point Dixon method for water-fat separation and computationally generates T1-weighted in- and out-of-phase fat and water images with the following parameters: repetition time (TR), 4.6 ms; first echo time (TE), 1.3 ms; second TE, 2.6 ms; slice thickness, 4.0 mm; flip angle, 12°; number of excitations, 1.0; matrix size, 300 by 200; field of view, 45.0 cm with an 80% phase field of view; and approximate acquisition time, 75 s. The parameters for single-shot fast-spin echo were as follows: TR/TE, 1,000/80; slice thickness, 6.0 mm; flip angle, number of excitations, 1.0; matrix size, 320 by 224; field of view, 38.0 cm; approximate acquisition time, 33 s.

Image Analysis

Image analysis was performed with an Advantage Workstation 4.7 (GE Healthcare) to evaluate the extent and location of [^{18}F]FDG uptake in the digestive tract both subjectively and objectively. Subjective analysis of the extent of [^{18}F]FDG uptake was conducted with the use of a 5-point visual scoring system by reference to the Deauville 5-point scale (D5PS) that is based on physiological [^{18}F]FDG uptake by the mediastinum and liver (15,16). The scores were defined as follows: 1, background level; 2, less than mediastinal physiological uptake (blood pool); 3, higher than mediastinal but lower than liver uptake; 4, slightly to moderately higher than liver uptake; and

Table 1—Characteristics of the metformin and control groups

Characteristic	Control group (n = 24)	Metformin group (n = 24)	P value
Age (years)	70.8 ± 9.3	69.6 ± 10.2	0.77
BMI (kg/m^2)	24.4 ± 5.4	24.5 ± 4.0	0.52
HbA_{1c} (%)	7.6 ± 1.2	7.5 ± 1.3	0.99
HbA_{1c} (mmol/mol)	59.1 ± 13.2	58.2 ± 14.7	
Sex (male/female)	13/11	14/10	0.77
FBG level on examination day (mg/dL)	151.3 ± 35.3	149.2 ± 33.0	0.82
Daily dose of metformin (mg)		750.0 ± 345.8	
Primary illness			
Pancreatic cancer	10 (41.7)	9 (37.5)	0.77
Pancreatitis	1 (4.2)	1 (4.2)	1
Colon cancer	2 (8.3)	1 (4.2)	1
Esophageal/stomach/duodenal cancer	1 (4.2)	1 (4.2)	1
Oral cancer	3 (12.5)	3 (12.5)	1
Uterine/ovarian cancer	3 (12.5)	3 (12.5)	1
Cholangiocarcinoma/gallbladder cancer	1 (4.2)	1 (4.2)	1
Liver cancer	0 (0.0)	2 (8.3)	0.49
Other	3 (12.5)	3 (12.5)	1
Antidiabetes medications other than metformin			
Glinide	0 (0.0)	0 (0.0)	
Dipeptidyl peptidase 4 inhibitor	12 (50.0)	19 (79.2)	0.035
Glucagon-like peptide 1 receptor agonist	1 (4.2)	1 (4.2)	1
Sulfonylurea	5 (20.8)	7 (29.2)	0.51
SGLT-2 inhibitor	0 (0.0)	3 (12.5)	0.23
α-Glucosidase inhibitor	4 (16.7)	4 (16.7)	1
Thiazolidinediones	0 (0.0)	2 (8.3)	0.49
Insulin	6 (25.0)	8 (33.3)	0.53

Data are means ± SD or n (%). FBG, fasting blood glucose.

5, substantially higher than liver uptake. The assessment was made separately by two readers (M.N. and F.Z., with 21 and 5 years, respectively, of experience in radiology and nuclear medicine) without access to patient history. The location of [^{18}F]FDG uptake was evaluated by the two readers on PET-MRI fusion images and was categorized according to four regions of the digestive tract: jejunum, ileum, right hemicolon, and left hemicolon.

Objective analysis of [^{18}F]FDG uptake in the digestive tract was performed by measurement of the maximum standardized uptake value (SUV_{max}) in segmented volumes of interest (VOIs) generated by MRI. The SUV on PET scans was calculated as previously described (29): SUV (g/mL) = tissue activity (Bq/mL)/[injected dose (Bq)/body weight (g)]. The VOIs were determined by signal intensities of T1- and T2-weighted MRI images (T1WI and T2WI, respectively), as previously described (30). In brief, fat images of the Dixon sequence were segmented by thresholding the signal intensity of the surrounding visceral fat (Supplementary Fig. 2*A*). T1WI and T2WI were then converted to nonfat images by subtraction of the segmented fat images (Supplementary Fig. 2*B* and *C*). T1WI and T2WI were also segmented by thresholding the signal intensity of the greater psoas muscle (Supplementary Fig. 2*D* and *E*), and the generated VOIs were finally copied to the PET images (Supplementary Fig. 2*F*) to extract the defined areas on PET (Supplementary Fig. 2*G*). Fused segmented PET and original MRI images (Supplementary Fig. 2*H*) were evaluated to determine SUV_{max} for each area of the digestive tract (Supplementary Fig. 2*I*).

The obtained data were categorized into two areas as follows: area 1, low T1WI and low T2WI; area 2, low T1WI and high T2WI or high T1WI and low T2WI (Supplementary Table 1). Area 1 of the digestive tract was assumed to correspond to the wall of the intestine—in particular, the muscle layer of the wall—and area 2 to intestinal fluid or stool.

Statistical Analysis

Data are presented as means ± SD. Differences between groups were evaluated with the Student t test or the Wilcoxon signed rank test for normally or nonnormally distributed data, respectively. The Tukey-Kramer honestly significant difference test was applied to compare parameters for each region of intestine between the two groups. The χ^2 test or Fisher exact test was applied for comparisons of categorical data. All statistical analysis was performed with the use of JMP Statistical Database Software version 13.0.0 (SAS Institute, Cary, NC). A P value of <0.05 was considered statistically significant.

RESULTS

Propensity score matching identified 24 pairs of subjects who were receiving treatment with metformin (metformin group) or not (control group) (Supplementary Fig. 1). There was no significant difference between the two groups in age, BMI, HbA_{1c} level, sex distribution, fasting blood glucose concentration on the day of examination, primary illness, or antidiabetes medications other than metformin, with the exception of dipeptidyl peptidase 4 inhibitor administration (Table 1). In the metformin group, the

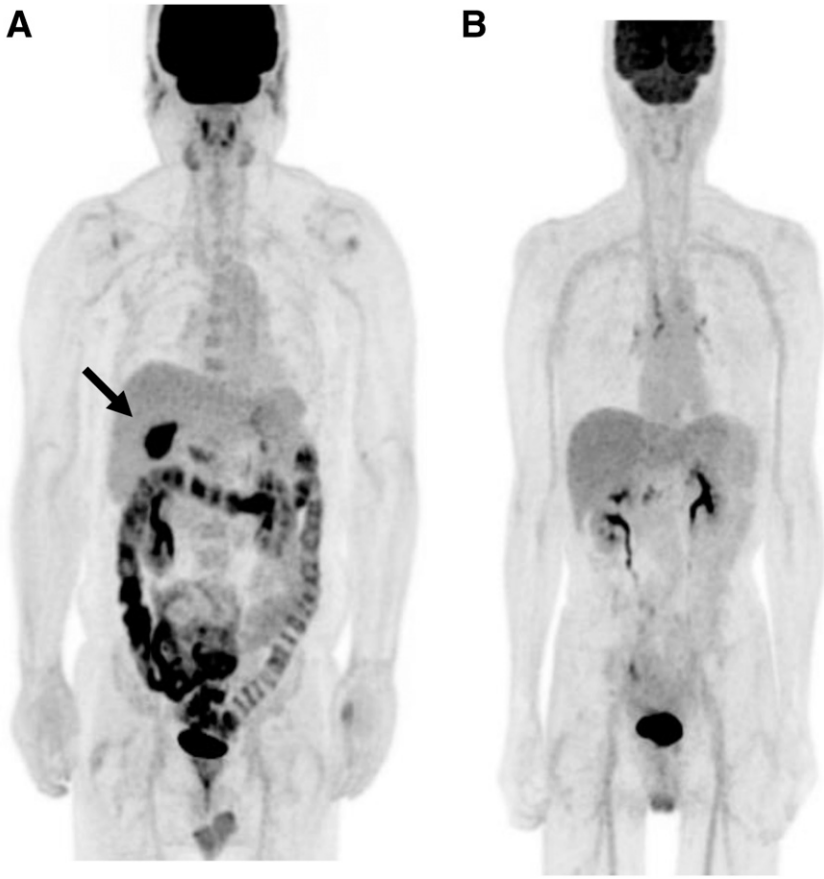

Figure 1—Representative [^{18}F]FDG PET images of subjects in the metformin (*A*) and control (*B*) groups. The arrow indicates gallbladder cancer, the primary illness of this patient.

average dosage of metformin was 750.0 ± 345.8 mg/day.

Representative [^{18}F]FDG PET images for subjects with high (metformin group) or low (control group) accumulation of [^{18}F]FDG in the intestine are shown in Fig. 1. The former subjects manifested accumulation of the tracer in the distal small intestine and colon, consistent with previous observations (15,16). Images for all of the study subjects are shown in Supplementary Fig. 3. Whereas the accumulation of [^{18}F]FDG in the intestine was also apparent in a few subjects of the control group (Supplementary Fig. 3*A*), the extent of the accumulation was greater in most cases in the metformin group (Supplementary Fig. 3*B*).

We first evaluated [^{18}F]FDG accumulation in each part of the intestine on the basis of SUV_{max}, a frequently adopted semiquantitative measure for such accumulation in a specific area (15,28). Whereas SUV_{max} for the ileum was significantly greater than that for the jejunum in the control group, SUV_{max} for the ileum, right hemicolon, or left hemicolon was significantly greater than that for the jejunum in the metformin group (Fig. 2*A*). SUV_{max} for all four parts of the intestine was significantly greater in the metformin group than in the control group (Fig. 2*A*), consistent with previous observations (15,28).

Visual analysis with the visual scoring system performed by two experienced radiologists yielded essentially identical results, with the average score for [^{18}F]FDG accumulation in the ileum, right hemicolon, or left hemicolon being significantly greater in the metformin group than in the control group (Fig. 2*B* and *C*).

We finally analyzed the accumulation of [^{18}F]FDG in the intestinal wall and intraluminal space separately. Area 1 (low T1WI and low T2WI) and area 2 (low T1WI and high T2WI, or high T1WI and low T2WI) were assumed to correspond to the intestinal wall (the muscle layer of the intestinal wall) and to bowel fluid or stool, respectively. SUV_{max} of area 1 did not differ between the metformin and control groups for any of the four parts of the intestine (Fig. 3*A*), suggesting that metformin does not stimulate the accumulation of [^{18}F]FDG in the intestinal wall. On one hand, SUV_{max} of area 1 was significantly greater for the left hemicolon than for the jejunum in the control group, whereas it was significantly greater for the right or left hemicolon than for the jejunum in the metformin group (Fig. 3*A*). On the other hand, SUV_{max} of area 2 for the ileum, right hemicolon, or left hemicolon was significantly greater in the metformin group than in the control group (Fig. 3*B*). SUV_{max} in area 2 was significantly greater for the ileum than for the jejunum in the control group, whereas it was significantly greater for the ileum, right hemicolon, or left hemicolon than for the jejunum in the metformin group (Fig. 3*B*). These results thus suggested that metformin promotes the release of [^{18}F]FDG into the intraluminal space of the intestine.

CONCLUSIONS

Taking advantage of the accurate registration and high soft-tissue contrast of PET-MRI, we were able to show here that metformin treatment is associated with an increase in [^{18}F]FDG accumulation in the intraluminal space, but not in the luminal wall, of the intestine. Our findings thus suggest that metformin stimulates the transport of glucose from the circulation into the intraluminal space of the intestine. Although metformin has been shown to exert various effects on the gut (6,7), the ability to promote the release of glucose into the intraluminal space has not previously been described.

We found that the metformin-associated increase in the accumulation of [^{18}F]FDG in the intraluminal space of the intestine was apparent for the ileum and colon but not for the jejunum, suggesting that the release of the tracer into the intraluminal space occurs not through biliary tracts but through the intestinal mucosa. In enterocytes, sodium–glucose cotransporter (SGLT) 1 and GLUT2 are expressed at the apical and basolateral surfaces, respectively, with the former mediating the uptake of glucose from the intraluminal space and the latter the transport of glucose into the circulation (31). However, metformin

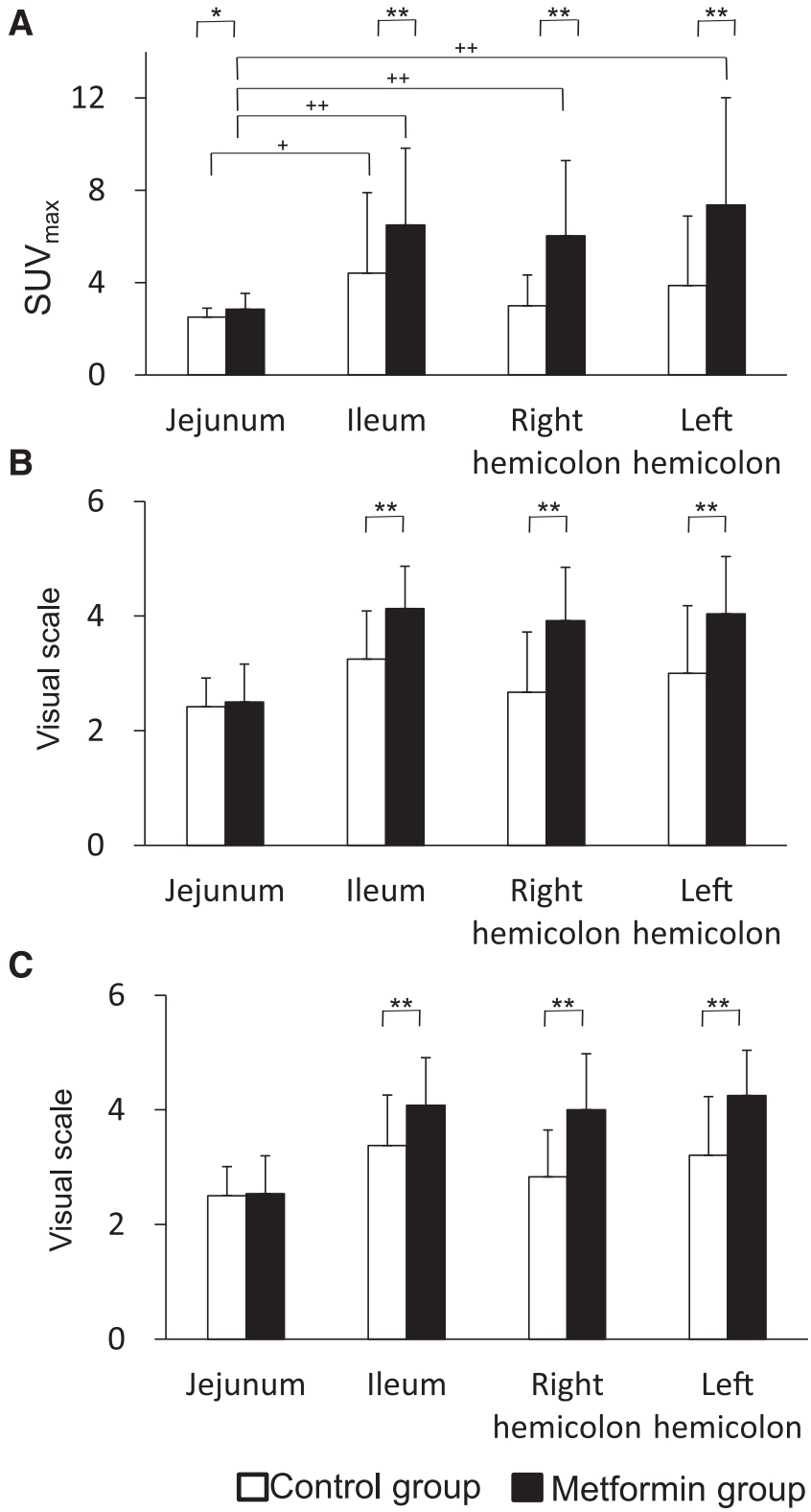

Figure 2—SUV_{max} (*A*) and visual scale scoring by two different observers (*B* and *C*) for each region of the intestinal tract in the metformin and control groups. Data are means ± SD ($n = 24$). *$P < 0.05$, **$P < 0.01$ (Student *t* test); +$P < 0.05$, ++$P < 0.01$ (Tukey-Kramer test).

has been shown to increase the abundance of GLUT2 at the apical surface of enterocytes both in vivo (32) and ex vivo (33), possibly via a 5′-AMPK–dependent mechanism (33,34). Given that transport of glucose via GLUT2 is bidirectional (35), it is possible that this transporter mediates the release of glucose from enterocytes into the intraluminal space. The translocation of GLUT2 to the apical surface might thus contribute to the metformin-induced release of glucose from enterocytes into the intraluminal space. Previous studies have shown that metformin stimulates the utilization of glucose in the intestine (36,37) via anaerobic metabolism (38). If metformin-induced glucose release is mediated via a GLUT2-dependent mechanism, it is likely that the concentration of glucose in enterocytes should be high enough to generate an outward gradient to the intraluminal space despite the enhanced metabolism. The molecular mechanism of how glucose is secreted into the intraluminal space in response to metformin remains to be elucidated.

Another important yet undetermined issue concerns the amount of glucose released into the intraluminal space in response to metformin. In the current study, we analyzed PET-MRI images obtained according to a routine method used mostly for the detection of tumors and then evaluated the radioactivity in the intestinal wall and intraluminal space on the basis of SUV_{max}. SUV_{max} is frequently adopted for assessment of the accumulation of radioactivity in a specific area of the body (28,29); however, it is a semiquantitative measure and does not fully reflect the total absolute amount of radioactivity in the area. Quantitation of the total absolute amount of radioactivity in the intestinal compartment will require the application of a nonroutine method for PET-MRI, such as that used for PET-MRI enterography (39). SGLT-2 inhibitors, the newest class of antidiabetes drugs, promote the transport of 10s to >100 g of glucose per day into urine (40). Quantitative analysis of metformin-induced glucose transport should provide insight into whether the phenomenon uncovered in the current study is related to the glucose-lowering effect of this drug.

One limitation of our study is its relatively small number of subjects. Moreover, whereas we applied propensity score matching to extract pairs of subjects, the retrospective nature of the study does not allow definitive conclusions to be drawn. SUV_{max} of small organs, such as the intestinal wall, is sometimes underestimated due to

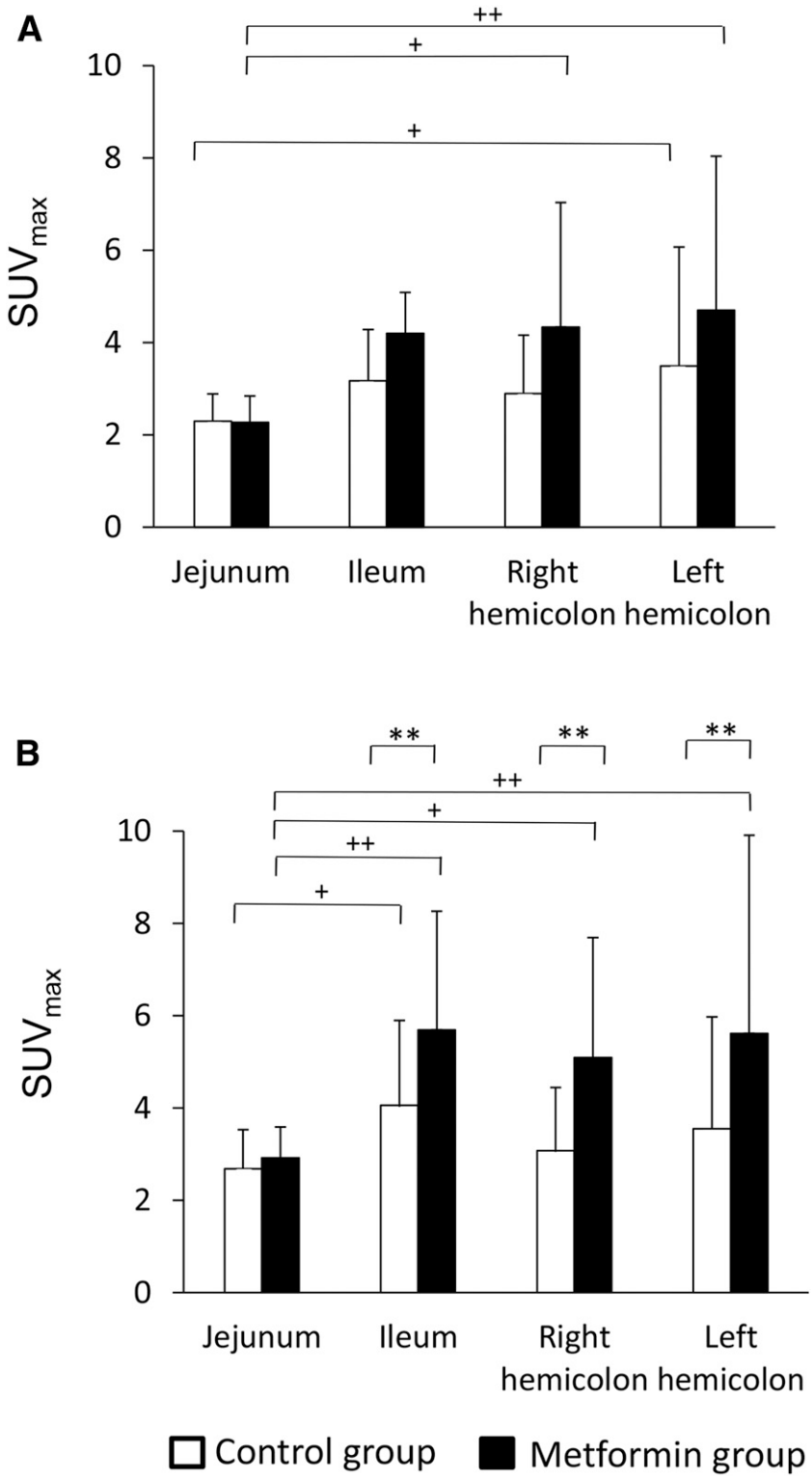

Figure 3—SUV_{max} for the intestinal wall (*A*) and intestinal contents (*B*) for each region of the intestinal tract in the metformin and control groups. Data are means ± SD. $^{**}P < 0.01$ (Student *t* test); $+P < 0.05$, $++P < 0.01$ (Tukey-Kramer test).

uncorrelated partial volume effects. Furthermore, given that it is difficult to separate completely the signal of the intestinal wall from those of bowel fluid or stool in close contact with the wall surface, we cannot exclude the possibility of spillover of the signals between the wall and intraluminal space. In addition, whereas [^{18}F]FDG PET is adopted not only for the detection of tumors but also for the evaluation of glucose uptake and thereby for that of the function of normal organs or tissues, such as brown adipose tissue (41,42), it is not known whether the dynamics of [^{18}F]FDG in the living body are identical to those of glucose. Given that most images were taken to detect tumors, we cannot completely exclude the possibility that the enhanced accumulation of FDG in tumors affected the imaging of the intestine to some extent.

In conclusion, we have here found that metformin treatment is associated with an increase in the accumulation of FDG in the intraluminal space of the ileum and colon, suggesting that this drug promotes the release of glucose into stool. A prospective study with a nonroutine imaging method that allows the quantitative analysis of total absolute radioactivity in the intestine will be required to clarify the clinical relevance of this novel pharmacological phenomenon.

Acknowledgments. The authors thank Hisako Komada, Natsu Otowa-Suematsu, Tomoko Yamada, and Hiroshi Miura (all from Kobe University Graduate School of Medicine) for helpful discussion.

Duality of Interest. K.Sa. and Y.O. have received lecture fees from Dainippon-Sumitomo Pharma, Novartis, Takeda Pharmaceutical, and Sanwa Kagaku Kenkyusho Co. Ltd. Y.T. has received lectures fees from Dainippon-Sumitomo Pharma, Novartis, and Takeda Pharmaceutical. W.O. has received research support from Dainippon-Sumitomo Pharma, Novartis, and Takeda Pharmaceutical as well as lecture fees from Dainippon-Sumitomo Pharma, Novartis, Takeda Pharmaceutical, and Sanwa Kagaku Kenkyusho Co. Ltd. No other potential conflicts of interest relevant to this article were reported.

Author Contributions. Y.M., M.N., and F.Z. contributed to collection, analysis, and interpretation of data. Y.M., K.Sa., Y.O., Y.T., and W.O. wrote the paper. M.N. and W.O. conceived and designed the study. Y.H. and K.Su. contributed to discussion. T.M. contributed to editing of the final manuscript. All authors reviewed the manuscript critically for intellectual content and approved the final version. W.O. is the guarantor of this work and, as such, had full access to all the data in the study and takes responsibility for the integrity of the data and the accuracy of the data analysis.

References

1. Miller RA, Chu Q, Xie J, Foretz M, Viollet B, Birnbaum MJ. Biguanides suppress hepatic glucagon signalling by decreasing production of cyclic AMP. Nature 2013;494:256–260

2. Madiraju AK, Erion DM, Rahimi Y, et al. Metformin suppresses gluconeogenesis by inhibiting mitochondrial glycerophosphate dehydrogenase. Nature 2014;510:542–546
3. Hunter RW, Hughey CC, Lantier L, et al. Metformin reduces liver glucose production by inhibition of fructose-1-6-bisphosphatase. Nat Med 2018;24:1395–1406
4. Madiraju AK, Qiu Y, Perry RJ, et al. Metformin inhibits gluconeogenesis via a redox-dependent mechanism in vivo. Nat Med 2018;24:1384–1394
5. Rena G, Hardie DG, Pearson ER. The mechanisms of action of metformin. Diabetologia 2017;60:1577–1585
6. McCreight LJ, Bailey CJ, Pearson ER. Metformin and the gastrointestinal tract. Diabetologia 2016;59:426–435
7. Minamii T, Nogami M, Ogawa W. Mechanisms of metformin action: in and out of the gut. J Diabetes Investig 2018;9:701–703
8. Czyzyk A, Tawecki J, Sadowski J, Ponikowska I, Szczepanik Z. Effect of biguanides on intestinal absorption of glucose. Diabetes 1968;17:492–498
9. Horakova O, Kroupova P, Bardova K, et al. Metformin acutely lowers blood glucose levels by inhibition of intestinal glucose transport. Sci Rep 2019;9:6156
10. Duca FA, Côté CD, Rasmussen BA, et al. Metformin activates a duodenal Ampk-dependent pathway to lower hepatic glucose production in rats. Nat Med 2015;21:506–511
11. Wu H, Esteve E, Tremaroli V, et al. Metformin alters the gut microbiome of individuals with treatment-naive type 2 diabetes, contributing to the therapeutic effects of the drug. Nat Med 2017;23:850–858
12. Sun L, Xie C, Wang G, et al. Gut microbiota and intestinal FXR mediate the clinical benefits of metformin. Nat Med 2018;24:1919–1929
13. Rigo P, Paulus P, Kaschten BJ, et al. Oncological applications of positron emission tomography with fluorine-18 fluorodeoxyglucose. Eur J Nucl Med 1996;23:1641–1674
14. Gontier E, Fourme E, Wartski M, et al. High and typical ^{18}F-FDG bowel uptake in patients treated with metformin. Eur J Nucl Med Mol Imaging 2008;35:95–99
15. Bahler L, Stroek K, Hoekstra JB, Verberne HJ, Holleman F. Metformin-related colonic glucose uptake; potential role for increasing glucose disposal?–A retrospective analysis of (18)F-FDG uptake in the colon on PET-CT. Diabetes Res Clin Pract 2016;114:55–63
16. Koffert JP, Mikkola K, Virtanen KA, et al. Metformin treatment significantly enhances intestinal glucose uptake in patients with type 2 diabetes: results from a randomized clinical trial. Diabetes Res Clin Pract 2017;131:208–216
17. Cho SY. To hold or not to hold metformin for FDG PET scans: that is the question. Radiology 2018;289:426–427
18. Massollo M, Marini C, Brignone M, et al. Metformin temporal and localized effects on gut glucose metabolism assessed using ^{18}F-FDG PET in mice. J Nucl Med 2013;54:259–266
19. Fraum TJ, Fowler KJ, McConathy J. PET/MRI: emerging clinical applications in oncology. Acad Radiol 2016;23:220–236
20. Kwon HW, Becker AK, Goo JM, Cheon GJ. FDG whole-body PET/MRI in oncology: a systematic review. Nucl Med Mol Imaging 2017;51:22–31
21. Fraum TJ, Ludwig DR, Hope TA, Fowler KJ. PET/MRI for gastrointestinal imaging: current clinical status and future prospects. Gastroenterol Clin North Am 2018;47:691–714
22. Pellino G, Nicolai E, Catalano OA, et al. PET/MR versus PET/CT imaging: impact on the clinical management of small-bowel Crohn's disease. J Crohns Colitis 2016;10:277–285
23. Fidler JL, Goenka AH, Fleming CJ, Andrews JC. Small bowel imaging: computed tomography enterography, magnetic resonance enterography, angiography, and nuclear medicine. Gastrointest Endosc Clin N Am 2017;27:133–152
24. Hoeffel C, Mulé S, Romaniuk B, Ladam-Marcus V, Bouché O, Marcus C. Advances in radiological imaging of gastrointestinal tumors. Crit Rev Oncol Hematol 2009;69:153–167
25. Erturk SM, Mortelé KJ, Oliva MR, Barish MA. State-of-the-art computed tomographic and magnetic resonance imaging of the gastrointestinal system. Gastrointest Endosc Clin N Am 2005;15:581–614, x
26. Ozülker T, Ozülker F, Mert M, Ozpaçaci T. Clearance of the high intestinal ($^{18)}$F-FDG uptake associated with metformin after stopping the drug. Eur J Nucl Med Mol Imaging 2010;37:1011–1017
27. Lee SH, Jin S, Lee HS, Ryu JS, Lee JJ. Metformin discontinuation less than 72 h is suboptimal for F-^{18} FDG PET/CT interpretation of the bowel. Ann Nucl Med 2016;30:629–636
28. Hamidizadeh R, Eftekhari A, Wiley EA, Wilson D, Alden T, Bénard F. Metformin discontinuation prior to FDG PET/CT: a randomized controlled study to compare 24- and 48-hour bowel activity. Radiology 2018;289:418–425
29. Lowe VJ, Hoffman JM, DeLong DM, Patz EF, Coleman RE. Semiquantitative and visual analysis of FDG-PET images in pulmonary abnormalities. J Nucl Med 1994;35:1771–1776
30. Im HJ, Paeng JC, Cheon GJ, et al. Feasibility of simultaneous 18F-FDG PET/MRI for the quantitative volumetric and metabolic measurements of abdominal fat tissues using fat segmentation. Nucl Med Commun 2016;37:616–622
31. Drozdowski LA, Thomson AB. Intestinal sugar transport. World J Gastroenterol 2006;12:1657–1670
32. Ait-Omar A, Monteiro-Sepulveda M, Poitou C, et al. GLUT2 accumulation in enterocyte apical and intracellular membranes: a study in morbidly obese human subjects and ob/ob and high fat-fed mice. Diabetes 2011;60:2598–2607
33. Sakar Y, Meddah B, Faouzi MA, Cherrah Y, Bado A, Ducroc R. Metformin-induced regulation of the intestinal D-glucose transporters. J Physiol Pharmacol 2010;61:301–307
34. Walker J, Jijon HB, Diaz H, Salehi P, Churchill T, Madsen KL. 5-aminoimidazole-4-carboxamide riboside (AICAR) enhances GLUT2-dependent jejunal glucose transport: a possible role for AMPK. Biochem J 2005;385:485–491
35. Zhao FQ, Keating AF. Functional properties and genomics of glucose transporters. Curr Genomics 2007;8:113–128
36. Pénicaud L, Hitier Y, Ferré P, Girard J. Hypoglycaemic effect of metformin in genetically obese (fa/fa) rats results from an increased utilization of blood glucose by intestine. Biochem J 1989;262:881–885
37. Bailey CJ, Mynett KJ, Page T. Importance of the intestine as a site of metformin-stimulated glucose utilization. Br J Pharmacol 1994;112:671–675
38. Wilcock C, Bailey CJ. Sites of metformin-stimulated glucose metabolism. Biochem Pharmacol 1990;39:1831–1834
39. Goldenberg JM, Cárdenas-Rodríguez J, Pagel MD. Preliminary results that assess metformin treatment in a preclinical model of pancreatic cancer using simultaneous [^{18}F]FDG PET and acidoCEST MRI. Mol Imaging Biol 2018;20:575–583
40. Vallon V, Thomson SC. Targeting renal glucose reabsorption to treat hyperglycaemia: the pleiotropic effects of SGLT2 inhibition. Diabetologia 2017;60:215–225
41. Saito M, Okamatsu-Ogura Y, Matsushita M, et al. High incidence of metabolically active brown adipose tissue in healthy adult humans: effects of cold exposure and adiposity. Diabetes 2009;58:1526–1531
42. Cypess AM, Lehman S, Williams G, et al. Identification and importance of brown adipose tissue in adult humans. N Engl J Med 2009;360:1509–1517